Thermally Developing Flow in an Annulus with a Boiling Boundary

S. K. Shin* and D. M. France†
University of Illinois at Chicago, Chicago, Illinois

Heat transfer from a liquid flowing in an annulus to a boiling fluid flowing in a tube was analyzed using four general formulations and several variations of them. The degree of complexity varied significantly among these analysis methods due primarily to the assumption of thermally fully developed flow applied in some methods and not in others. Measurements from a sodium-heated boiling water experiment provided the boundary conditions for the annulus heat-transfer problem. Finite-difference techniques were employed in some of the analyses, and an appropriate inverse heat-transfer technique was included in one of them. Comparisons of heat-transfer parameters calculated from the analysis methods are presented and the accuracies assessed. Three of these methods compared favorably with the most complete and complex of the analyses considered.

Nomenclature

C_p	= specific heat, J/kg K
D	= diameter, m
$f(r)$	= initial sodium temperature distribution at $z = 0$, °C
h	= heat transfer coefficient, W/m² K
k	= thermal conductivity, W/m K
k_e	= effective turbulent thermal conductivity, W/m K
M	= mass flowrate, kg/s
q	= heat flux at tube inner surface, W/m²
r	= radial coordinate measured from centerline of water tube, m
T	= temperature, °C
TSAT	= saturation temperature, °C
TWALL	= temperature at D_i (wall i.d. temperature), °C
V	= axial velocity, m/s
z	= axial coordinate in direction of sodium flow, m
ρ	= density, kg/m³
Subscripts	
b	= bulk fluid
i	= tube inner surface (wall i.d.)
o,w	= tube outer surface
s	= shell

Introduction

THERMALLY developing single phase flow in an annulus with arbitrary thermal boundary conditions is a general case of the classical Graetz problem. An important application occurs in the area of experimental two-phase flow where the boundary condition is not arbitrary but rather imposed by a boiling fluid. A class of problems in this area is related to steam generators for application to liquid metal cooled nuclear reactors (LMR). The geometry of interest consists of high-pressure water boiling inside of long vertical tubes heated by a liquid metal, usually sodium, flowing countercurrently outside of the tubes. In an experimental situation, measurements made in the heating fluid are used to determine important conditions in the boiling fluid including heat transfer rates, heat transfer coefficients, and flow regime transitions such as critical heat flux, bulk boiling, and superheating. The purpose of this investigation was to develop and compare several types of analyses of heat transfer from a liquid metal flowing in an annulus with boundary conditions generated from a boiling fluid. Four general analysis types were considered, including several variations of them, which ranged significantly in complexity. Heat transfer predictions were compared among the analyses, and the boundary conditions used were obtained from experimental measurements.

Experimental development programs simulating steam generators with liquid metal heating have been performed in many countries. In the U.S., large-scale experiments were performed in the test facility at the Energy Technology Engineering Center (ETEC). The most recent tests[1] employed a full-scale LMR steam generator tested at 70 MW maximum input. Earlier tests in a 28 MW unit were reported in Ref. 2. Smaller-scale sodium-heated experiments in the 1 MW range have been performed by Westinghouse,[3,4] General Electric[5] and Argonne National Laboratory.[6] Experiments outside of the U.S. have also ranged in size up to about 50 MW inputs. A recent article[7] summarizes ten years of large-scale sodium-heated steam generator testing and serves as an example of this work.

Several types of analyses have been used by experimenters to determine local heat flux profiles from temperature measurements in liquid-heated systems. Other parameters of interest are generally obtainable after the heat flux has been calculated. The analyses investigated in this study have all been used in some form by experimenters in analyzing experimental data. Differences in parameter magnitudes and trends among the analyses were quantified. Since the analyses differ considerably in complexity, the results presented are useful in optimizing the choice of analysis for a specific system or set of experiments.

Analyses

The analysis of experimental data from fluid-heated systems generally commences with the calculation of the heat flux profile from temperature measurements as discussed in the Introduction. The four analysis types considered in this investigation are specifically for determining that heat flux profile. (Subsequently, tube or boiling fluid temperatures may be calculated.) For the purpose of discussion, these four types have been given the identification labels "gradient," "coefficient," "developing," and "explicit" methods. All four methods have been applied to the case of a straight tube, shell, and tube steam generator. For the purpose of comparison with data, a single

Received March 13, 1987; revision received Sept. 15, 1987. Copyright © American Institute of Aeronautics and Astronautics, Inc., 1987. All rights reserved.

*Graduate Research Assistant, Department of Mechanical Engineering.

†Associate Professor, Department of Mechanical Engineering.

tube was analyzed with water boiling inside heated by sodium flowing countercurrently in a surrounding annulus. The analyses were directly applied to the annular sodium flow bounded on the inside by the water tube on the outside by the sodium shell as shown in Fig. 1. Measurements of sodium flow rate and axial shell temperatures were the inputs to the calculations.

The conservation of energy for steady flow of sodium in the annulus is

$$\rho C_p V \frac{\partial T}{\partial z} = k_e \left(\frac{\partial^2 T}{\partial r^2} + \frac{1}{r} \frac{\partial T}{\partial r} \right) + \left(\frac{\partial k_e}{\partial r} \frac{\partial T}{\partial r} \right) \tag{1}$$

where axial conduction was neglected. The flow was assumed to be turbulent and the quantities $T(r,z)$ and $V(r)$ are the time-averaged temperature and axial velocity, respectively. All four models assumed that the flow was hydrodynamically fully developed. The initial condition at the sodium inlet was

$$T(r,o) = f(r) \tag{2}$$

where $f(r)$ was constant for uniform inlet temperature. The boundary conditions came from the measured shell temperatures, T_s, (assumed to be at the inside shell diameter, D_s) and from the insulated condition of the shell

$$T\left(\frac{D_s}{2}, z\right) = T_s(z) \tag{3}$$

$$\left.\frac{\partial T}{\partial r}\right|_{r=\frac{D_s}{2}} = 0 \tag{4}$$

[Measured shell heat loss may be incorporated into Eq. (4), but it is small for a well-insulated shell.] The heat flux at the inside surface of the water tube was written in terms of the sodium bulk temperature as

$$q = \frac{MC_p}{\pi D_i} \frac{dT_b}{dz} \tag{5}$$

Gradient Method 1

This analysis is the simplest of the four methods used. It involves the most assumptions, and it is potentially the least accurate. The method is distinguished by the assumption of a thermally fully developed condition where the heat flux is determined directly from the shell gradient (hence the name gradient method). Equation (5) was replaced by

$$q = \frac{MC_p}{\pi D_i} \frac{dT_s}{dz} \tag{6}$$

and Eq. (1) was not solved. After calculating the heat flux by Eq. (6), two approaches were used for determining parameters in the tube wall and the boiling fluid. The simplest of these approaches employed a heat transfer coefficient for the sodium obtained from experimental investigations in annuli. Under the further assumption that the shell temperature and sodium bulk temperature are approximately equal, a second simple relation was obtained relating the tube wall temperature to the shell temperature.

$$q = \frac{hD_o}{D_i}(T_o - T_s) \tag{7}$$

Gradient Method 2

The second approach applied to the gradient analysis method did not rely on the input of an empirical heat transfer coefficient. Equations (1) and (5) were combined under the assumptions of thermally fully developed flow and uniform velocity,

$$\frac{1}{r}\left(\frac{\partial}{\partial r}\right)\left(r\frac{\partial T}{\partial r}\right) = \frac{D_i q}{k\left[\left(\frac{D_s}{2}\right)^2 - \left(\frac{D_o}{2}\right)^2\right]} \tag{8}$$

For constant heat flux q in axial increment dz, Eq. (8) was integrated twice with boundary conditions (3) and (4), to yield the radial sodium temperature distribution. Evaluating the result at the shell yielded a relationship that was applied in place of Eq. (7)

$$T_o = T_s + \frac{D_i q}{4k}\left[\frac{2\ell n \frac{D_s}{D_o}}{1 - \left(\frac{D_o}{D_s}\right)^2} - 1\right] \tag{9}$$

The bulk temperature was then given by

$$T_b = T_s + \frac{D_i q}{8k}\left[\frac{1 - \left(\frac{D_o}{D_s}\right)^4 + 4\left(\frac{D_o}{D_s}\right)\ell n \frac{D_o}{D_s}}{\left[1 - \left(\frac{D_o}{D_s}\right)^2\right]^2}\right] \tag{10}$$

Both approaches used with the gradient analysis method have the common feature of calculating heat flux from the shell temperature gradient, Eq. (6). Forms of the gradient method were used in the sodium-heated tests of Ref. 4 and the mercury-heated tests of Ref. 8. This study considered the two forms presented, gradient methods 1 and 2, and the empirical heat transfer coefficient of Ref. 9 was used with Eq. (7).

Coefficient Method 1

A coefficient type analysis was used in conjunction with the experiments reported in Ref. 5. The improvement in this method over the gradient analysis is the use of Eq. (5) for the heat flux rather than Eq. (6). As in the simplest form of the gradient analysis, a sodium heat transfer coefficient taken from Ref. 9 was used, but it was applied in the usual way

$$q = h\frac{D_o}{D_i}(T_o - T_b) \tag{11}$$

The assumption that the shell and bulk temperatures are equal was not made, but it was assumed that the system was fully developed thermally and that the radial velocity profile was uniform. Seven variations of this method were considered. All of them used a sodium heat transfer coefficient in calculating the heat flux. In this first case, backward finite difference was applied to Eq. (5).

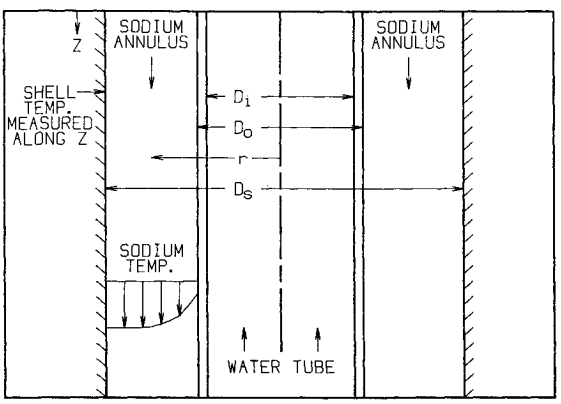

Fig. 1 Annulus geometry.

$$q_{j+1} = \frac{MC_p}{\pi D_i}\left[\frac{T_{b_{j+1}} - T_{b_j}}{\Delta z}\right] \tag{12}$$

Combining Eq. (11) with the gradient model result relating tube wall and shell temperatures, Eq. (9), yielded an expression for the bulk temperature.

$$T_b = T_s + \frac{D_i q}{4k}\left[\frac{2\ell n \frac{D_s}{D_o}}{1-\left(\frac{D_o}{D_s}\right)^2} - 1 - \frac{4k}{hD_o}\right] \tag{13}$$

Equations (12) and (13) were solved iteratively for the bulk temperature T_b and the heat flux, q as in the studies of Ref. 5.

Coefficient Method 2

The approach used in this method involved solving the same equations as the coefficient method 1, Eqs. (9), (11), and (12), without the need for an iterative solution scheme. Equation (13) was evaluated at $j+1$ and combined with Eq. (12),

$$T_{b_{j+1}} = \frac{T_{b_j} - \delta\,\Delta z\, T_{s_{j+1}}}{1 - \delta\,\Delta z} \tag{14}$$

where

$$\delta = \frac{4\pi k}{MC_p\left[\frac{2\ell n \frac{D_s}{D_o}}{1-\left(\frac{D_o}{D_s}\right)^2} - 1 - \frac{4k}{hD_0}\right]} \tag{15}$$

Since the shell temperatures were experimentally measured, and thus known at all j, the bulk temperature at $j+1$ was found from Eq. (14) knowing T_{b_j}. The heat flux was then found by combining Eqs. (12) and (14).

$$q_{j+1} = \frac{MC_p}{\pi D_i}\left[\frac{T_{b_j} - T_{s_{j+1}}}{1 - \delta\,\Delta z}\right] \tag{16}$$

Then combining Eq. (16) with Eq. (9) gave the tube wall temperature at $j+1$.

$$T_{o_{j+1}} = T_{s_{j+1}} + \frac{D_i}{4k}\left[\frac{2\ell n \frac{D_s}{D_o}}{1-\left(\frac{D_o}{D_s}\right)^2} - 1\right] q_{j+1} \tag{17}$$

Equations (14), (16), and (17) represent the desired solution, and no iteration scheme was required.

Coefficient Method 3

The third approach used with the coefficient method was to solve Eqs. (5), (9), and (11) where the differential form, Eq. (5), was used instead of the difference form, Eq. (12). A closed-form solution was obtained assuming the shell temperature to be linear in increment Δz. Combining Eq. (5) with Eq. (13) [which came from Eqs. (9) and (11)] gave

$$\frac{dT_b}{dz} - \delta T_b = -\delta T_s(z) \tag{18}$$

Integrating Eq. (18) over Δz gave the bulk temperature

$$T_{b_{j+1}} = T_{s_j} + \left[T_{b_j} - T_{s_j} + \frac{T_{s_j} - T_{s_{j+1}}}{\delta\,\Delta z}\right]\exp[\delta\,\Delta z] - [1 + \delta\,\Delta z]\left[\frac{T_{s_j} - T_{s_{j+1}}}{\delta\,\Delta z}\right] \tag{19}$$

The heat flux was obtained from Eqs. (5), (18), and (19).

$$q_{j+1} = \frac{MC_p\delta}{\pi D_i}\left[-\frac{T_{s_j} - T_{s_{j+1}}}{\delta\,\Delta z} + \left\{\frac{T_{s_j} - T_{s_{j+1}}}{\delta\,\Delta z} - (T_{s_j} - T_{b_j})\right\}\exp[\delta\,\Delta z]\right] \tag{20}$$

The tube wall temperature at $j+1$ was obtained directly from Eq. (9) once the heat flux was found from Eq. (20).

Coefficient Method 4

Introduction of Eq. (11) to the fully developed treatment of gradient method 2 produced an extra degree of freedom in the problem. Coefficient methods 1–3 utilized Eqs. (5), (9), and (11). Coefficient method 4 followed the approach of coefficient method 3 but used Eqs. (5), (10), and (11). The shell temperature was assumed to be linear in increment Δz, and the following differential equation was obtained.

$$\frac{dT_b}{dz} - \Lambda T_b = -\Lambda T_s \tag{21}$$

where

$$\Lambda = \frac{8\pi k}{MC_p}\left[\frac{\left[1-\left(\frac{D_o}{D_s}\right)^2\right]^2}{1-\left(\frac{D_o}{D_s}\right)^4 + 4\left(\frac{D_o}{D_s}\right)^2 \ell n \frac{D_o}{D_s}}\right] \tag{22}$$

Equation (21) has the same form as Eq. (18) with δ replaced by Λ, and the wall temperature was obtained from Eqs. (10), (11), and the equivalent of Eq. (20) using Λ in place of δ.

$$T_{o_{j+1}} = T_{s_{j+1}} + \frac{D_i q_{j+1}}{8k} F \tag{23}$$

where

$$F = \frac{1-\left(\frac{D_o}{D_s}\right)^4 + 4\left(\frac{D_o}{D_s}\right)^2 \ell n \frac{D_o}{D_s}}{\left[1-\left(\frac{D_o}{D_s}\right)^2\right]^2} + \frac{8k}{hD_o} \tag{24}$$

Coefficient Method 5

The approach was the same as coefficient method 2 using backwards finite differencing, but Eqs. (5), (10), and (11) were solved instead of Eqs. (5), (9), and (11).

Coefficient Method 6

The experimental data, to which the analysis methods will be compared in subsequent sections, was smoothed using cubic spline functions. Therefore, the approach of coefficient method 3 was followed using a cubic function for the shell temperature in each Δz increment which represented the smoothed data precisely.

Coefficient Method 7

The analysis method also used cubic functions, but Eqs. (5), (10), and (11) were solved instead of Eqs. (5), (9), and (11) as in coefficient method 6. This method followed the approach of coefficient method 4 but cubic functions were used for the shell temperatures instead of linear functions.

Developing Method

The developing analysis is the most complete of the four general methods considered. The axial heat flux distribution may exhibit large gradients in liquid-heated boiling systems. Consequently, the heating fluid does not generally become fully developed thermally. This method treats the heating fluid

(sodium) as developing thermally over the entire heat transfer length (hence the name developing method). A form of this method was used in the analysis of experimental data presented in Ref. 6. Equation (1) was solved numerically with initial condition, Eq. (2), and boundary conditions, Eqs. (3) and (4). A turbulent velocity distribution, $V(r)$, was used following the work of Ref. 10. The relationship between the eddy diffusivities of heat and momentum was obtained from the model of Refs. 11 and 12. Although the velocity $V(r)$ was not an explicit function of axial distance z it varied in that direction as fluid properties changed with temperature. The same was true for k_e, which varied radially as a function of fluid temperature.

The inclusion of both turbulent effects and thermally developing conditions made the solution to the energy equation of this analysis considerably more involved than the previous two methods presented. The developing method was further complicated by the fact that both boundary conditions, Eqs. (3) and (4), were specified at the same radial location. Solution to the energy Eq. (1) under these conditions is a problem of the inverse type, and the treatment of Ref. 13 was applied.

Explicit Method

Heat transfer problems of the inverse type may on occasion be solved by standard finite-difference formulations. Equation (1) with boundary conditions (3) and (4) was subjected to semi-implicit and explicit finite-difference formulations, and the latter produced some stable results. The assumptions employed in this method were uniform sodium velocity (slug flow) and negligible turbulent transport of heat. These two simplifications were guided by results from the developing analysis. Axial heat conduction was retained in the energy equation for this explicit analysis, and a central differencing scheme was employed with radial and axial increments chosen for numerical stability.

Application

The four analysis methods were applied to a test from Ref. 6. The test section geometry conformed to Fig. 1 where high-pressure water was boiled as it flowed upward inside the 13.1 m long tube heated by sodium flowing countercurrent in the annulus between the tube and shell. Shell temperatures were measured by 102 thermocouples spot welded to it, and fluid flowrates, test section inlet and exit temperatures, and water pressure were also measured. The water tube was $2\frac{1}{4}$ Cr-1 Mo steel with inside and outside diameters of 10.1 mm and 15.9 mm, respectively. The inside diameter of the type 304 stainless steel shell was 31.5 mm.

The test series reported in Ref. 6 included over 400 individual steady-state tests covering a large range of parameters. In view of the various assumptions involved with the four analyses, it was anticipated that the largest differences among them would occur in tests with large axial gradients in temperature and heat flux. Thus, test number R294 was selected for this investigation from the test series of Ref. 6 because the axial heat flux gradients were among the largest of all the tests. The test parameters were:

Water mass flux	= 2500 kg/m^{2}s
Water pressure	= 6.9 MPa
Water inlet temperature	= 215°C
Water outlet quality	= 0.49
Sodium mass flowrate	= 0.63 kg/s
Sodium inlet temperature	= 512°C
Sodium outlet temperature	= 249°C

The measured shell temperatures during this steady-state test are shown as circular symbols in Fig. 2. The solid line in Fig. 2 is the result of a cubic spline function curve fit to the measurements which formed the basis for all four analysis methods.

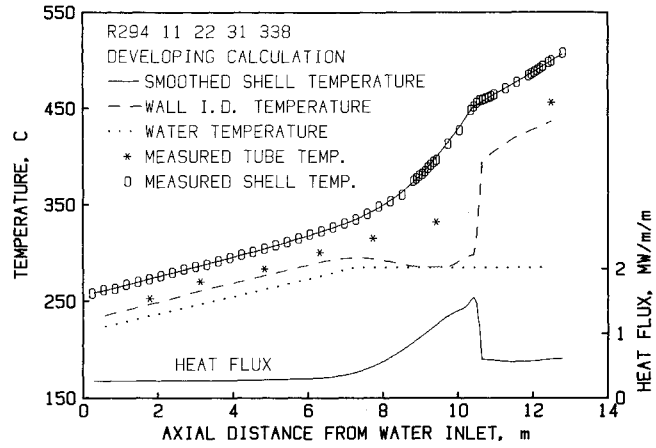

Fig. 2 Benchmark calculations.

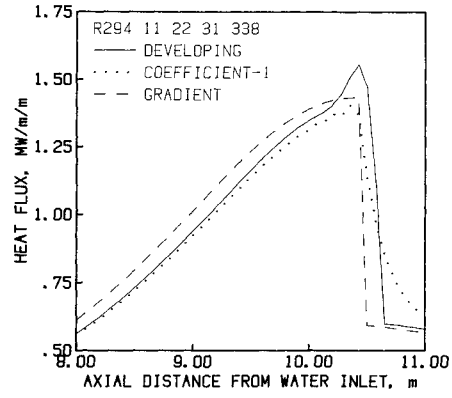

Fig. 3 Comparison of three general calculation methods.

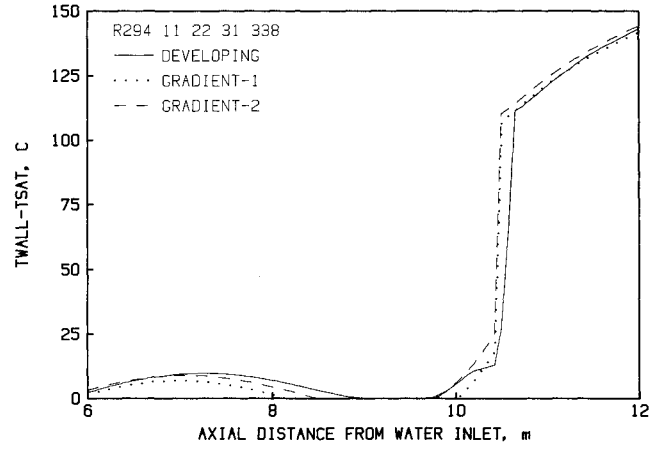

Fig. 4 Comparison of gradient calculation methods.

Results

Since the developing method was the most complete, the results of the other three methods were compared to it. Calculated parameters from the developing method of analysis are shown in Fig. 2 over the entire test section length. Consistency with experimental measurements is observed by comparing the measured wall temperatures within the tube wall to the calculated wall temperatures at the water tube inside surface. The relative magnitudes of these two wall temperatures acted as a general control on the calculations. The overall heat transfer predictions of the developing method have been found to be in

good agreement with experiments. Such comparisons were made for experiments similar to those of Ref. 6 in which the water exited the test section superheated, which provided an accurate measurement of the water heat gain.

The primary parameter for comparison among the analyses is the heat flux distribution along the length of the test section. The largest differences occurred in the peak region corresponding to critical heat flux (CHF) in the boiling water. A comparison is shown in Fig. 3 of peak heat flux results from three of the general methods: developing, coefficient and gradient. The gradient method results shown in Fig. 3 are the same for both variations studied, gradient methods 1 and 2, and the results of coefficient method 1 are representative of most of the coefficient analyses, methods 1–5. The results shown for these three general methods are considered to be in good overall agreement with two important local differences. First, the developing method shows a larger heat flux at CHF than either the gradient or coefficient methods. Considering the developing analysis results as the most accurate, the gradient and coefficient results at CHF are low by 10% and 12%, respectively. The second area of important differences among the results of these three methods appears in the transition boiling region beyond CHF. The heat flux gradients are largest in this region and are predicted differently by the three methods. Results from both the developing and gradient methods exhibit similarly large gradients although they differ in axial location by a small amount. The coefficient method, however, produced a boiling heat flux distribution at transition that has significantly smaller gradients and extends over a larger axial distance than the results of the other two methods. Care was taken to insure that numerical accuracy did not influence this result. The axial increment, dz, was identical in both the coefficient and developing analyses.

Results from the two variations of the gradient analysis method are compared in Fig. 4 using the important temperature difference for boiling. No significant difference is observed between the two variations of the gradient method, and agreement between them and the developing method is good.

Calculations from coefficient methods 1–5 were in very close agreement. A typical comparison is shown in Fig. 5. Essentially the only difference observed is the minor convergence stability problem that occurred in the CHF region of the iteration method, coefficient method 1.

Spline functions were applied to the experimental data in two sets, upstream and downstream, of CHF. This double spline application resulted in accurate representation of the shell temperatures and their gradients along the entire test section length. Use of a single set of spline functions had the general effect of reducing gradients especially in the CHF region. A comparison is shown in Fig. 6 of results from the developing method using single and double spline function sets. In this case, the CHF region gradients calculated from the single spline functions were not reduced significantly from the double spline results. This good comparison in the CHF region was obtained at the expense of the water inlet region where the single spline functions did not smooth the data sufficiently causing the axial heat flux oscillation shown in Fig. 6.

The fourth general method of analysis applied in this study was very sensitive to large gradient areas and, thus, to the use of single or double spline function sets for data smoothing. Employing the preferred double spline smoothing, as used with all other methods, produced an unstable condition in the large gradient CHF region as shown in Fig. 7 for the explicit-2 finite difference analysis. A stable solution was obtained when a single spline function set was employed, but gradients in the CHF region were reduced as shown in Fig. 7 as explicit-1. A semi-im-

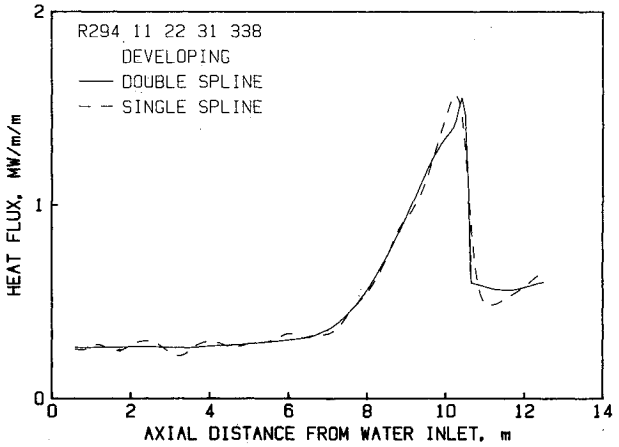

Fig. 6 Data smoothing.

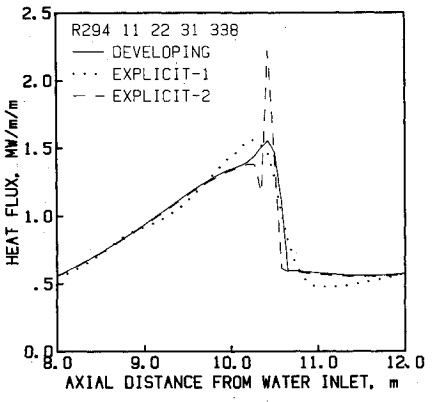

Fig. 7 Comparison of explicit calculations methods.

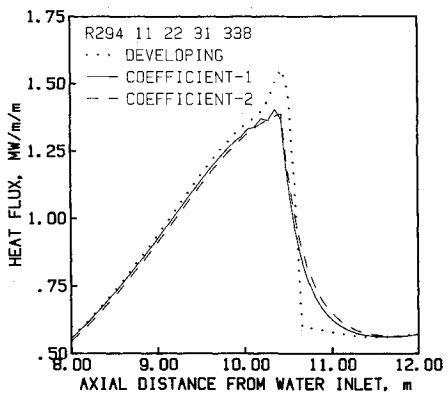

Fig. 5 Comparison of coefficient calculation methods.

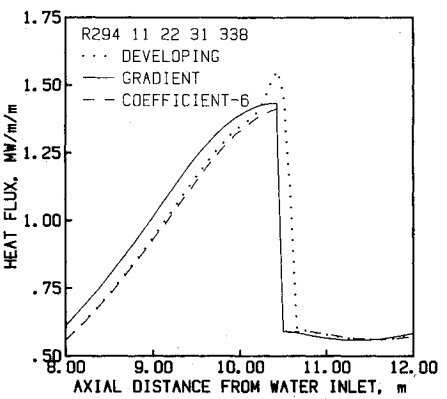

Fig. 8 Best calculation methods.

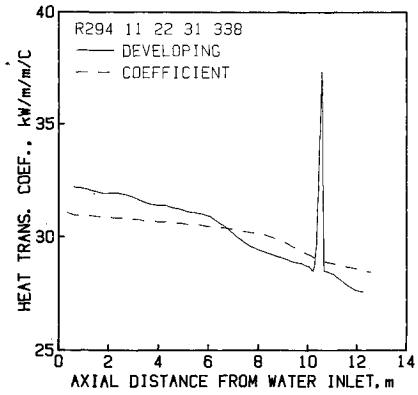

Fig. 9 Heat transfer coefficient in the annulus.

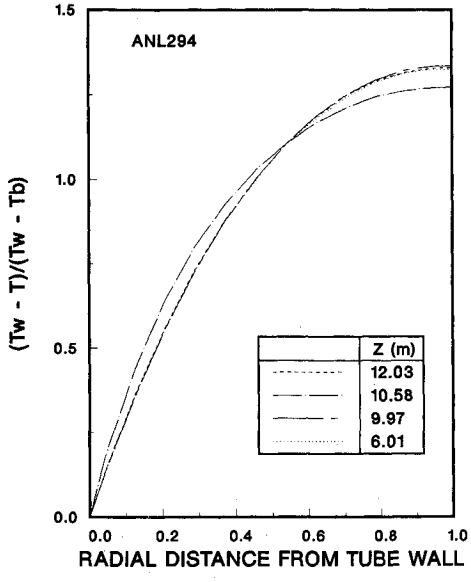

Fig. 10 Radial temperature distrubution in the annulus.

plicit finite-difference approach applied to test R294 produced no stable solutions.

Discussion

Three of the methods of analysis investigated agreed relatively well with calculations from the developing method. These methods, gradient and coefficient 6 and 7, preserved the large heat flux gradients in the transition boiling region although the peak heat fluxes compared with the developing method were low by about 10%. A comparison of these methods is shown in Fig. 8 where coefficient methods 6 and 7 produced nearly identical results. The relatively good agreement among these methods is somewhat surprising considering the numerous simplifications associated with the gradient and coefficient methods compared to the developing method. One major contribution to this agreement was the accuracy of the empirical heat transfer coefficient used in the heat flux calculation with the coefficient methods. The empirical coefficient from Ref. 9 is compared to the calculated values from the developing method in Fig. 9. The comparison is considered good except very close to CHF, downstream of the 10 m location.

The abrupt increase in sodium heat transfer coefficient shown in Fig. 9 is indicative of a departure from a thermally fully developed condition. This condition was investigated further by calculating the dimensionless radial temperature distribution across the annulus. The results are shown in Fig. 10 at four axial locations calculated using the developing method. The peak heat flux (CHF) occurred at 10.43 m, and the high gradient transition boiling region persisted downstream to 10.66 m. The dimensionless temperature distribution of Fig. 10 is invariant with axial position both upstream and downstream of the transition boiling region. However, a deviation is clearly seen within the transition boiling region at 10.58 m. This departure from the fully developed condition produced the poor heat transfer coefficient comparision in the transition boiling region shown in Fig. 9. However the length of this region is quite short and essentially thermally fully developed flow existed over 98% of the heat transfer length. This result was a second major contributor to the agreement among the methods shown in Fig. 8 since both the gradient and coefficient methods included the assumption of thermally fully developed flow.

Conclusions

The experimental data used in this study were selected for the very large thermal gradients encountered. Even in this case, three of the less detailed methods of analysis were found to produce favorable results when compared to the more complete developing analysis method. These three methods incorporated several simplifying assumptions, yet they predicted the large transition boiling gradients well, and the peak heat flux predictions were within 10–12%. The success of these methods was attributed to the flow being very close to the thermally fully developed condition which was an underlying assumption in the formulation of both the gradient and coefficient methods. Although neither the axial wall temperature or heat flux were uniform as shown in Fig. 2, the thermally fully developed condition was essentially disrupted only in the transition boiling region where gradients were maximum. The short axial length of this region did not impair the generally favorable results of the gradient method and coefficient methods 6 and 7. The importance of these results is accentuated by the significant reduction in complexity of application of these three methods compared to the developing method. All three methods were shown to be good choices for the problem presented, and gradient method 1 is considered to be preferable for extension of this work.

Considering a new application in the general area of this investigation, gradient method 1 is preferable to gradient method 2 because of the use of an experimental heat transfer coefficient in the former case. The coefficient can be specific to the application of interest. Gradient method 1 is also preferred to the coefficient methods for new applications, because gradient method 1 is not so sensitive to the data smoothing technique employed.

References

[1]Fox, C. H., Jr., Purcell, W. S., and Wieseneck, H. C., "CRBRP Stream Generator Testing Experience," *Liquid Metal Engineering and Technology,* Vol. 2, British Nuclear Energy Society, London, 1984, pp. 203–210.

[2]Harty, R. B., "Heat Transfer Performance of a Sodium Heated Stream Generator," *Proceedings of the 68th Annual AIChE Meeting*, Atlanta, GA, November 1975.

[3]Efferding, L. E., "Dynamic Stability Experimental/Analytical Program Results on a Multiple Tube Sodium Heated Stream Generator Model Employing Double Wall Tubes," American Society of Mechanical Engineers Paper 83-WA/NE-7, 1983

[4]Hwang, J. Y., Efferding, L. E., and Waszink, R. P., "Sodium-Heated Evaporator Critical Heat Flux Experiments at Subcritical Conditions for Commercial LMFBR Plant Application," American Society of Mechanical Engineers Paper 76-JPGC-NE-10, 1976.

[5]Wolf, S. and Holmes, D. H., "Critical Heat Flux in a Sodium-Heated Steam Generator Tube," *Proceedings of the 17th National Heat Transfer Conference*, August 1977.

[6]France, D. M., Carlson, R. D., Chiang, T., and Minkowycz, W. J., "Critical Heat Flux Experiments and Correlation in a Long, Sodium-Heated Tube," *Journal of Heat Transfer*, Vol. 103, February 1981, pp. 74–80.

[7]Fontaine, J. P. and Llory, M., "Ten Years of Steam Generator Tests on a 45 MW Sodium Test Loop," *Liquid Metal Engineering and Technology*, Vol. 2, British Nuclear Energy Society, London, 1984, pp. 217–224.

[8]France, D. M., "DNB in Liquid Metal Heated Forced Convection Boiling," *International Journal of Heat and Mass Transfer*, Vol. 16, 1973, pp. 2343–2354.

[9]Dwyer, O. E., "On the Transfer of Heat to Fluids Flowing Through Pipes, Annuli and Parallel Plates," *Nuclear Science and Engineering*, Vol. 17, 1963, pp. 336–344.

[10]Quarmby, A., "An Analysis of Turbulent Flow in Concentric Annuli," *Applied Science Research*, Vol. 19, July 1968, pp. 250–273.

[11]Deissler, R. G., "Analysis of Fully-Developed Turbulent Heat Transfer at Low Peclet Numbers in Smooth Tubes with Application to Liquid Metals," Res. Memo. E 52F05, National Adv. Comm. Aero., Washington, DC, 1952.

[12]Reynolds, A. J., "The Prediction of Turbulent Prandtl and Schmidt Numbers," *International Journal of Heat and Mass Transfer*, Vol. 18, 1975, pp. 1055–1069.

[13]Beck, J. V., "Nonlinear Estimation Applied to the Nonlinear Inverse Heat Conduction Problems," *International Journal of Heat and Mass Transfer*, Vol. 13, 1970, pp. 703–716.

From the AIAA Progress in Astronautics and Aeronautics Series . . .

TRANSONIC AERODYNAMICS—v. 81

Edited by David Nixon, Nielsen Engineering & Research, Inc.

Forty years ago in the early 1940s the advent of high-performance military aircraft that could reach transonic speeds in a dive led to a concentration of research effort, experimental and theoretical, in transonic flow. For a variety of reasons, fundamental progress was slow until the availability of large computers in the late 1960s initiated the present resurgence of interest in the topic. Since that time, prediction methods have developed rapidly and, together with the impetus given by the fuel shortage and the high cost of fuel to the evolution of energy-efficient aircraft, have led to major advances in the understanding of the physical nature of transonic flow. In spite of this growth in knowledge, no book has appeared that treats the advances of the past decade, even in the limited field of steady-state flows. A major feature of the present book is the balance in presentation between theory and numerical analyses on the one hand and the case studies of application to practical aerodynamic design problems in the aviation industry on the other.

Published in 1982, 669 pp., 6×9, illus., $39.95 Mem., $79.95 List

TO ORDER WRITE: Publications Dept., AIAA, 370 L'Enfant Promenade S.W., Washington, D.C. 20024-2518